Surface Energy and Surface Proton Order of Ice I*h*

Ding Pan,[1,2] Li-Min Liu,[2,3,4,5] Gareth A. Tribello,[4,5,6] Ben Slater,[4,5,6] Angelos Michaelides,[2,3,4,5,*] and Enge Wang[1,2]

[1]*Institute of Physics, Chinese Academy of Sciences, P.O. Box 603, Beijing 100190, China*
[2]*Fritz-Haber-Institut der Max-Planck-Gesellschaft, Faradayweg 4-6, 14195 Berlin, Germany*
[3]*London Centre for Nanotechnology, University College London, London WC1H 0AJ, United Kingdom*
[4]*Materials Simulation Laboratory, University College London, London WC1H 0AJ, United Kingdom*
[5]*Department of Chemistry, University College London, London WC1H 0AJ, United Kingdom*
[6]*Davy Faraday Research Laboratory, Kathleen Lonsdale Building, Gower Street, University College London, London WC1E 6BT, United Kingdom*

(Received 28 July 2008; revised manuscript received 4 September 2008; published 9 October 2008)

Ice I*h* is comprised of orientationally disordered water molecules giving rise to positional disorder of the hydrogen atoms in the hydrogen bonded network of the lattice. Here we arrive at a first principles determination of the surface energy of ice I*h* and suggest that the surface of ice is significantly more proton ordered than the bulk. We predict that the proton order-disorder transition, which occurs in the bulk at ~72 K, will not occur at the surface at any temperature below surface melting. An order parameter which defines the surface energy of ice I*h* surfaces is also identified.

DOI: 10.1103/PhysRevLett.101.155703 PACS numbers: 64.60.Cn, 68.47.−b, 82.65.+r

Ice I*h*, the normal form of ice, is built from water molecules arranged on a tetrahedral lattice, subject to a set of rules known as the ice rules [1]. These rules allow for orientational disorder of the molecules, which is discussed in terms of the positional disorder of the hydrogen atoms, a phenomenon known as proton disorder. Under ambient pressures, ice I*h* is the stable phase down to ~72 K [2], below which a proton ordered (ferroelectric) phase known as ice XI becomes the ground state. In practice, the ordering transformation from ice I*h* to the lowest total energy ice XI phase rarely happens since, as the temperature is lowered to the transition temperature, proton motion comes to a halt. This leaves the crystal out of equilibrium at below 72 K with residual entropy. Indeed, ice I*h* is so resistant to transforming from ice I*h* into ice XI that a dopant that accelerates proton rearrangement (KOH) is usually added to make it occur.

Given the experimental difficulties in probing the ice I*h*-XI transition, molecular simulations are very useful [3–5]. In particular, in a *tour de force* study, density functional theory (DFT) was combined with a framework based on graph invariants to simulate the bulk ice I*h*-XI transition. A transition temperature of 98 K was predicted, within 30 K of the experimental transition [5]. This demonstrates that DFT is appropriate for tackling the subtle question of proton order and disorder in ice, something which cannot necessarily be said about the many empirical potentials that otherwise describe many parts of the phase diagram of water well [6].

Unlike in bulk ice, the understanding of the energetics of proton order at the surface is in its infancy [7,8]. This is true despite widespread interest in ice surfaces at low temperatures, motivated mainly by their catalytic role in atmospheric chemistries such as ozone depletion (see, e.g., [9]). Indeed, the understanding is so incomplete that the value of the surface energy—one of the most important quantities of any material—is well-established neither experimentally nor theoretically and how it is influenced by proton order is not known. Here, in arriving at an *ab initio* determination of the surface energy of the (0001) (basal plane) of ice I*h*, we demonstrate that the energetics of proton ordering differs significantly at the surface compared to the bulk. Indeed, the range of energies spanned by proton ordered configurations is more than an order of magnitude larger than in bulk, implying a much higher order-disorder transition temperature at the surface compared to the bulk. Monte Carlo (MC) simulations with parametrized potentials support this suggestion, predicting no order-disorder transition below the onset of surface melting.

The DFT calculations reported here have been performed with the CP2K/QUICKSTEP program, which employs a hybrid Gaussian and plane-wave basis set [10]. The Perdew, Burke, and Ernzerhof exchange-correlation functional has been used [11]. Core electrons are described with Goedecker, Teter, and Hutter pseudopotentials [12] and the valence electrons are expanded in terms of Gaussian functions with a triple-ζ doubly polarized basis set (TZV2P). For the auxiliary basis set of plane waves, a 340 Ry cutoff is used. A variety of bulk and surface structural models were employed, all with a minimum of 24 molecules per bilayer. MC simulations with an empirical potential were also performed [13]. The potential employed was a six site, rigid body, potential [14] modified to reproduce the DFT proton ordering energies of designated proton configurations.

First, we discuss our results for bulk ice I*h* and ice XI. Here we use 96 molecule cells to generate pseudorandom

ice configurations with Cota and Hoover's method [15], as further developed by Hayward and Reimers [16]. In addition, all ice I*h* structures considered have zero dipole moment along the (0001) (bilayer) plane. As well as the normal ice I*h* models, calculations on ferroelectric ice XI [$CmC2_1(mm2)$ space group] and antiferroelectric ice XI structures were performed. The lowest energy antiferroelectric model explored (structure 14 in Ref. [4], $P12_11$ space group) is fully proton ordered but has no dipole moment perpendicular to the (0001) basal plane unlike ferroelectric ice XI which, of course, does. For each of these classes of structure, the energy-volume equation of state curves were determined, such as those displayed in Fig. 1. Consistent with previous DFT studies with smaller simulation cells [3–5,17,18], ice XI has the largest cohesive energy E_{coh}. The next most stable phase is antiferroelectric ice XI and then the normal ice I*h* structures. For clarity in Fig. 1, only a single ice I*h* curve is displayed. However, several were calculated, and all have energies within 4 meV/H_2O. Thus, E_{coh} exhibits only a small dependence on the degree of proton order, with all structures (ice XI and all of the ice I*h* structures) being within $\sim$5 meV/H_2O. This energy range is consistent with the thermal energy available at the bulk transition temperature of $\sim$70 K ($k_BT \sim 5$ meV/H_2O).

We now explore the energetics of the (0001) basal plane of ice I*h* and ice XI [see Fig. 2(a)]. The key thermodynamic quantity of any surface is the surface energy γ, which is defined here as

$$\gamma = \frac{E_{\mathrm{tot}}^{\mathrm{slab}}(n) - nE_{\mathrm{tot}}^{\mathrm{slab}}}{A}, \qquad (1)$$

where $E_{\mathrm{tot}}^{\mathrm{slab}}$ is the total energy of the slab, n is the number of bilayers in the slabs, and A is the surface area of the two sides of the slab. Below, to allow direct comparison with bulk energies, we also consider surface energies per molecule in the upper half of each surface bilayer. The bulk reference per bilayer $E_{\mathrm{tot}}^{\mathrm{bulk}}$ is extracted from calculations on ice slabs from the relation $E_{\mathrm{tot}}^{\mathrm{bulk}} = E_{\mathrm{tot}}^{\mathrm{slab}}(n) - E_{\mathrm{tot}}^{\mathrm{slab}}(n-1)$.

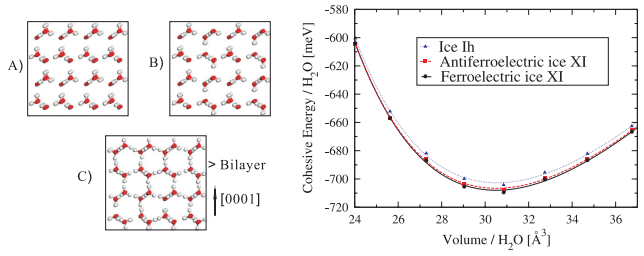

FIG. 1 (color online). Structures and energies of bulk ice XI and I*h*. Left: Illustration of certain unit cells used for the bulk calculations all containing 96 molecules: (A) ferroelectric ice XI; (B) antiferroelectric ice XI; and (C) a regular ice I*h* cell. Right: Energy-volume curves for the three selected bulk structures shown on the left. The energies of the bulk structures with different proton arrangements are all within $\sim$5 meV/H_2O.

This relation is valid when the slab is sufficiently thick that the bilayer insertion energy is equivalent to the addition of a bilayer of bulk ice. For the surfaces examined here, γ is rather insensitive to the number of layers used and, as can be seen from Fig. 2(b), is converged already at 2–3 bilayers. γ has been computed for ferroelectric and antiferroelectric ice XI and >20 ice I*h* structures. Consistent with previous studies and, of course, because it possesses a dipole along the surface normal, the ferroelectric ice XI surface is unstable [8,19]. A value of 12.2 meV/Å^2 [205 meV/(H_2O in the top half bilayer)] is obtained for the surface energy of antiferroelectric ice XI (we note that this resembles Fletcher's striped phase [7]). For ice I*h*, however, we do not get a unique value for γ. Instead, a range of values is obtained, at the lower end of which is the surface energy of antiferroelectric ice XI. This is not entirely unexpected since, as we know, the cohesive energy of bulk ice depends on the degree of proton disorder within the simulation cell. The interesting finding here is that the variation of γ with the degree of proton order by far exceeds the small range in the bulk. Specifically, for the structures considered here, the variation with proton order in the bulk is $\sim$5 meV/H_2O, whereas at the surface it is as much as 100 meV per H_2O molecule in the top half of each bilayer.

Can the large range of values for γ_{Ih} be understood? Drawing on studies of water clusters [20] and the work on the surface of ice by Fletcher [7] and Buch *et al.* [8], we

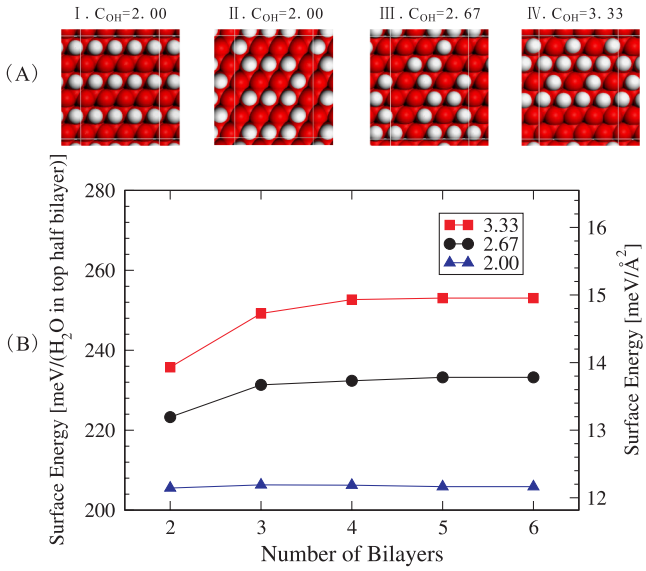

FIG. 2 (color online). Structures and energies of ice surfaces with different arrangements of dangling OH groups. (A) Top view of the (0001) basal plane of selected ice I*h* models with order parameters of (I) 2.00, (II) 2.00, (III) 3.33, and (IV) 2.67. Red balls represent oxygen atoms and white balls hydrogen atoms, which are enlarged here to emphasize the proton arrangement at each surface. (B) Surface energies of models I, III, and IV as a function of the number of bilayers in the slabs.

anticipate that the upright OH groups in the top half bilayer at the surface, those which "dangle" out of the surface, might play an important role. To distinguish different distributions of the dangling OH bonds, we define an order parameter:

$$C_{\mathrm{OH}} = \frac{1}{N_{\mathrm{OH}}} \sum_{i=1}^{N_{\mathrm{OH}}} c_i, \tag{2}$$

where N_{OH} is the number of dangling OH bonds for each slab and c_i is the number of nearest neighbor dangling OH bonds around the ith dangling OH bond. Note that the nearest neighbor site for one dangling OH group beside another corresponds to the next nearest neighbor site of the hexagonal O lattice. The order parameter C_{OH} quantifies the average separation between the dangling OH groups at the surface: The larger C_{OH}, the more inhomogeneous the distribution of the dangling OH groups. A fully random arrangement will have a value of $C_{\mathrm{OH}} = 3$. The smallest possible value of C_{OH} for a nonpolar surface is 2, which corresponds to, among other structures, those resembling antiferroelectric ice XI surfaces. Remarkably, we find that when the γ's of the many surfaces considered here are plotted as a function of C_{OH} a linear relationship is observed. This is displayed in Fig. 3, where it can also be seen that the lowest energy surfaces are those with $C_{\mathrm{OH}} = 2$. The fact that this is a true surface effect can be further seen by the absence of a dependence of C_{OH} on the bulk energies extracted from each slab. For the lowest value of the order parameter $C_{\mathrm{OH}} = 2$, we have computed 6 structures which all have γ's within 0.5 meV/ Å^2 or 8 meV per H_2O in the top half bilayer of each other. Some of these $C_{\mathrm{OH}} = 2$ surfaces correspond to Fletcher's striped phase [e.g., (I) in Fig. 2(a)] and some do not [e.g., (II) in Fig. 2(a)]. Therefore, although it is clear that the lowest energy surfaces are those with $C_{\mathrm{OH}} = 2$, it is not yet prudent to designate any one particular termination as "the" lowest energy structure of the ice surface.

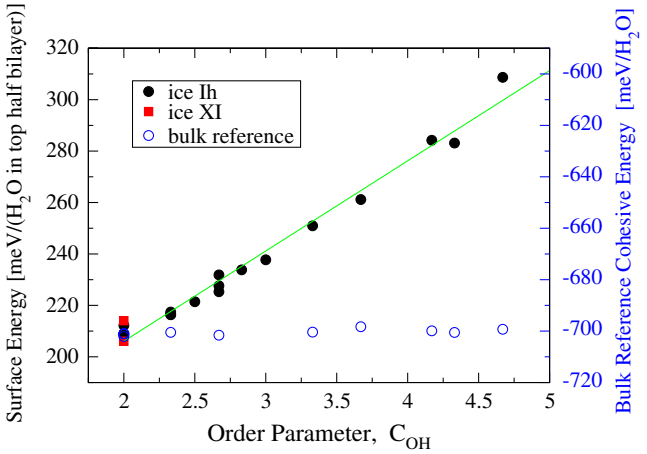

FIG. 3 (color online). Surface energies of ice Ih and antiferroelectric ice XI versus C_{OH}. A strong dependence on C_{OH} is observed, whereas for reference almost no dependence of the energy of bulk ice on C_{OH} is found (right axis). A fully proton disordered surface corresponds to $C_{\mathrm{OH}} = 3$, whereas we see here that the lowest energy structures have $C_{\mathrm{OH}} = 2$.

A classical electrostatics model proves useful to understand the strong dependence of γ_{Ih} on the proton arrangement at the surface. Specifically, we write γ for the various ice Ih surfaces γ_{Ih} as

$$\gamma_{Ih} \approx \gamma_{C_{\mathrm{OH}}=2} + \frac{\Delta E_{\mathrm{HH}}}{A}, \tag{3}$$

where $\gamma_{C_{\mathrm{OH}}=2}$ is the surface energy of surfaces with $C_{\mathrm{OH}} = 2$ and ΔE_{HH} is a surface excess energy which $C_{\mathrm{OH}} > 2$ surfaces have due to the additional repulsion between dangling OH groups brought about by their on average closer proximity to each other. We express the *total* repulsion between dangling OH groups E_{HH} through a screened Coulomb interaction, which leads to

$$\gamma_{Ih} \approx \gamma_{C_{\mathrm{OH}}=2} + \frac{q^2}{4 d_{\mathrm{HH}} \sigma}(C_{\mathrm{OH}} - 2), \tag{4}$$

an expression for γ_{Ih} which depends linearly on C_{OH} with a slope proportional to q^2, where q is the "effective charge" on the H atoms of the dangling OH groups. If d_{HH} is set to 4.42 Å—taken from our computed nearest neighbor distances at the ice surface—and σ is the area per molecule in the top half bilayer (16.92 Å^2), then the best fit value for the charge is $0.21e$ [see Fig. 3] [21]. This appears to be a physically reasonable value of the effective charge on the hydrogen atoms, coming within the range of (0.03–0.43) obtained upon performing Löwdin and Mulliken population analyses of the DFT electron densities of the ice surfaces. The nearest neighbor description of the stabilities of ice surfaces arrived at here is the essence of the model employed in the pioneering study of Fletcher [7], and it is remarkable to see such a simple correlation come out of the sophisticated first principles simulations.

We now consider the implications of this result to the ice XI-Ih transition with the aid of MC simulations with an empirical potential. So as to access a large range of temperatures including unrealistically high temperatures (40–500 K) without the "complications" of melting in the MC

TABLE I. Monte Carlo results on the variation of C_{OH} with temperature. Results are averaged over the two faces of a six bilayer slab. Layer 1 is the external surface (top half bilayer). The variance within each layer is given in parenthesis.

T (K)	Layer 1	Layer 2	Layer 3
40	2.00 (0.000)	2.42 (0.041)	2.44 (0.007)
100	2.00 (0.000)	2.48 (0.020)	2.58 (0.026)
200	2.13 (0.003)	2.70 (0.022)	2.75 (0.028)
500	2.33 (0.011)	2.71 (0.020)	2.74 (0.023)

simulations, structural relaxation effects such as displacements of the water molecules from their lattice sites were not considered; i.e., the focus was uniquely on proton reorientation and the influence this alone has on the free energies of the slabs. The key conclusion of these simulations is that, at all temperatures below the melting point, the surfaces remain with an order parameter close to $C_{OH} = 2$ (see Table I). Indeed, upon specifically passing through the bulk order-disorder transition temperature (72 K), no additional disorder is introduced at the surface with C_{OH} remaining at 2.00. Even at an unrealistically high temperature of 500 K, the surface is still far from being fully disordered, possessing a value of only $C_{OH} = 2.33$ [22]. Thus, overall, the MC simulations reveal that there is insufficient thermal energy available to access many of the distinct proton configurations at the surface, and therefore an order-disorder transition equivalent to the one in bulk ice does not take place at the surface at any temperature before the crystal melts.

In conclusion, the surface energy of ice I*h* has been computed from first principles, revealing that the energetics of proton ordering differs markedly at the surface compared to that in the bulk. The main implication of this is that under equilibrium the ice I*h* surface will not become fully proton disordered at any relevant temperature. We note that Buch *et al.* [8] came to a similar conclusion based on simulations with empirical potentials and, moreover, concluded that the lowest energy surfaces were those which corresponded to Fletcher's striped phase [(I) in Fig. 2]. This is an interesting and appealing suggestion. However, it cannot be fully substantiated by the present *ab initio* results. Here we find that other $C_{OH} = 2$ surfaces such as the one shown in (II) in Fig. 2 have similar energies. Therefore, it is not yet possible to say with confidence if any one particular structure is the lowest energy structure. The related observation reported herein that the stabilities of individual surfaces is governed by electrostatic repulsion between dangling OH groups is also likely to have implications to, for example, the premelting of ice. Although the microscopic mechanisms involved in premelting are complex and not fully understood, involving a breakdown in the hexagonal lattice of water molecules, we suggest that regions on the surface with high concentrations of dangling OH groups will melt first. Substantiating this will provide interesting work for the future, requiring systematic studies of the dependence of melting on C_{OH}. However, MD simulations suggest that the onset of premelting is indeed sensitive to surface proton distribution [23]. Likewise, it is plausible that other properties of the ice surface, such as sticking probabilities for molecular and dissociative adsorption, will be sensitive to the degree of local order. Finally, on a technical point, having established that the energetics of proton order differs significantly at the surface compared to the bulk, it is no longer recommended to apply Hayward and Reimers [16] rules alone for choosing bulk ice I*h* simulation cells from which surface structures are to be generated. Surface structures with C_{OH} much higher than 2.0—such as the fully random bulk I*h* value of $C_{OH} = 3$—will lead to unrealistically high energy, proton clustered surfaces with physicochemical properties that differ from the true structure.

D. P. and E. W. are supported by NSFC. E. W. is also supported by an Alexander von Humboldt research grant and A. M. by the EURYI scheme [24] and the EPSRC. We are grateful to M. Scheffler for supporting the early stages of this work and to P. J. Feibelman for reading the manuscript. Computational resources from the London Centre for Nanotechnology are warmly acknowledged.

*angelos.michaelides@ucl.ac.uk

[1] J. D. Bernal and R. H. Fowler, J. Chem. Phys. **1**, 515 (1933).
[2] S. Kawada, J. Phys. Soc. Jpn. **32**, 1442 (1972).
[3] G. A. Tribello and B. Slater, Chem. Phys. Lett. **425**, 246 (2006).
[4] T. K. Hirsch and L. Ojamäe, J. Phys. Chem. B **108**, 15 856 (2004).
[5] C. Knight *et al.*, Phys. Rev. E **73**, 056113 (2006).
[6] E. Sanz, C. Vega, J. L. Abascal, and L. G. MacDowell, Phys. Rev. Lett. **92**, 255701 (2004).
[7] N. H. Fletcher, Philos. Mag. B **66**, 109 (1992).
[8] V. Buch *et al.*, Proc. Natl. Acad. Sci. U.S.A. **105**, 5969 (2008).
[9] M. J. Molina *et al.*, Science **238**, 1253 (1987).
[10] J. Vande Vondele *et al.*, Comput. Phys. Commun. **167**, 103 (2005).
[11] J. P. Perdew, K. Burke, and M. Ernzerhof, Phys. Rev. Lett. **77**, 3865 (1996).
[12] S. Goedecker, M. Teter, and J. Hutter, Phys. Rev. B **54**, 1703 (1996).
[13] The Metropolis MC simulations were performed on 6 bilayer slabs with 160 molecules per bilayer. Simulations were run for $\geq 500\,000$ steps, and the mean and variance were collected over the final 15 000 accepted moves.
[14] H. Nada and J. P. van der Eerden, J. Chem. Phys. **118**, 7401 (2003).
[15] E. Cota and W. G. Hoover, J. Chem. Phys. **67**, 3839 (1977).
[16] J. A. Hayward and J. R. Reimers, J. Chem. Phys. **106**, 1518 (1997).
[17] S. J. Singer *et al.*, Phys. Rev. Lett. **94**, 135701 (2005).
[18] S. Casassa *et al.*, Chem. Phys. Lett. **409**, 110 (2005).
[19] G. Bussolin, S. Casassa, C. Pisani, and P. Ugliengo, J. Chem. Phys. **108**, 9516 (1998).
[20] J.-L. Kuo *et al.*, J. Chem. Phys. **118**, 3583 (2003).
[21] The mean square error of this linear fit is 3.7 meV/(H_2O in the top half bilayer), which is smaller than the spread in the DFT data at given values of C_{OH}.
[22] The MC simulations reveal that by the second and third layers larger values of C_{OH} are observed (Table I).
[23] C. L. Bishop *et al.*, Faraday Discuss. (to be published).
[24] http://www.esf.org/euryi.